Longqiu Shao ✉
Qinghua Zhang
Gaowei Lei
Naiquan Su
Penghui Yuan

https://doi.org/10.21278/TOF.462032721
ISSN 1333-1124
eISSN 1849-1391

A DIMENSIONLESS IMMUNE INTELLIGENT FAULT DIAGNOSIS SYSTEM FOR ROTATING MACHINERY

Summary

Aiming at the shortcomings of the traditional frequency domain analysis method, such as failure to find early faults, the misjudgement and omission of fault types, and failure to diagnose complex faults, a new approach is developed, which is different from the existing technical route in the field of fault diagnosis, by closely following real-time online, intelligent and accurate requirements in the field of monitoring and fault diagnosis of large rotating machinery. Combining immune mechanism, dimensionless index, support vector machine and other artificial intelligence technologies, linked with the particularity of fault diagnosis problems, a fault diagnosis classification algorithm based on memory sequence is proposed, and an intelligent fault diagnosis system based on a dimensionless immune detector and support vector machine was developed. Finally, the system was applied to a compressor unit in a petrochemical enterprise and good results were achieved.

Key words: *rotating machinery, dimensionless index, on-line monitoring, fault diagnosis*

1. Introduction

A large rotating machinery unit is a complex engineering system, which sets higher requirements for the reliability and safety of the large equipment structure, and for the process and operating state [1-3]. Rotating machinery fault diagnosis technology provides a scientific basis for timely and effective maintenance and health management of the system by monitoring, analysing, judging and separating the fault types of the system in a complex environment. Consequently, this technology has good prospects for application in aviation, aerospace and other fields with high safety requirements [3, 4]. In particular, rotating mechanical equipment (such as rotating bearings, steam turbines, compressors, fans, etc.) is key equipment in petroleum, chemical, metallurgy, machinery manufacturing, aerospace and other important engineering fields [5-8]. In these areas, research on the fault diagnosis method of this kind of equipment has always been a hot spot. Królczyk et al. [9] reported on the state of the art and recent advancements in the fault diagnosis of rotating machines.

In a complex environment, vibration monitoring signals of large rotating machinery sets often have a large number of nonlinear and random information, which raises great difficulties in the analysis of fault signals [2, 10]. Considering that vibration time-domain signals are the most basic and original signals, it will be very beneficial to maintain the basic characteristics of signals if fault features can be extracted directly through such time-domain signals for fault diagnosis [10]. In time-domain analysis, the probability density function of vibration signals can better reflect the fault information. By means of the probability density function of vibration signals, dimensional indicators (such as mean value, root mean square value, etc.) and dimensionless indicators (such as waveform index, margin index, pulse index, etc.) in the amplitude range have now been derived [4]. In practice, although the dimensional index is sensitive to fault characteristics and its value will rise with the development of the fault, it will also change due to the change of working conditions (such as load, speed, etc.), and it is easily affected by disturbance, so its performance is not stable [11]. In contrast, the dimensionless index is not sensitive to disturbance in the vibration monitoring signal and its performance is relatively stable [12]. In particular, these dimensionless indicators are insensitive to changes in the amplitude and frequency of the signal, that is, they have little to do with the working conditions of the machine. Therefore, the dimensionless index has been widely used in the fault diagnosis of rotating machinery [13]. Among the dimensionless indicators, the kurtosis index and the pulse index are more sensitive to impact faults. Especially in the early stage of fault occurrence, the pulse with a large value is relatively small, and the other index values do not increase much. However, the kurtosis index and the pulse index rise rapidly [14], so these two indexes are more sensitive to the early faults of rotating machinery. However, for rotating machinery operating under actual working conditions, its faults are usually compound faults, that is, the fault of the equipment is the result of multiple single faults [14]. Existing relevant studies mainly focus on the treatment of single faults [9, 15, 16], while the diagnosis of complex faults is still at the primary stage, and relevant studies are also very scarce. Therefore, the research and development of a more efficient and reliable intelligent fault diagnosis system is of great significance to ensure the safe production of modern petrochemical enterprises.

An intelligent fault diagnosis system generally consists of a fault information base, diagnosis reasoning mechanism, interface and database. Lu et al. [17] constructed an unsupervised intelligent fault diagnosis system based on feature transfer to extract the historical labeled data of the source domain, using feature transfer to facilitate the fault diagnosis of the target domain. Wang et al. [18] designed an artificial intelligent fault diagnosis system of complex electronic equipment based on a BP neural network to address the system diagnosis problem of qualitative fault data and encountered problems of low accuracy and time-consuming fault detection. Hu et al. [19] proposed an intelligent fault diagnosis system based on the whole integrated framework, and conducted investigations in a case study of process plants in a petrochemical corporation. Hao et al. [20] designed a distributed monitoring and intelligent diagnosis system for large-scale electro-hydraulic devices, based on the utilization of information fusion technology. As a result of using information fusion methods at the multi-sensor data level, feature level and decision-making level, both precision and real-time performance of condition monitoring and fault diagnosis have been greatly improved, leading to an advance in the accuracy of monitoring and diagnosis.

2. Key technology

The biology immune system is a system with the ability of pattern recognition, distributed detection, memory capacity, self-learning, diversity, etc. The artificial immune system is a new discipline with strong vitality based on the features of the biology immune system to solve problems encountered in practical application and projects. The negative selection algorithm which derives from the mechanism of recognizing the self and non-self of the immune system

provides a new idea and methods in the field of fault diagnosis. Two important terms frequently used when discussing the immune system are antigens and antibodies. As you can imagine, antigens are foreign substances (e.g., hepatitis viruses), and antibodies are the soldiers of the immune system that fight them. When antigens (such as the hepatitis B antigen) infect the body, the immune system produces corresponding antibodies, namely hepatitis B antibodies. Antibodies bind to antigens and remove them from the body, making the body immune to the hepatitis B virus. In the intelligent fault diagnosis system, the dimensionless immune detector (antibody) is used to diagnose the fault type (antigen).

2.1 Dimensionless index

The dimensionless index is composed of the ratio of two quantities with the same dimension, which has a certain physical significance when describing a specific system. The dimensionless diagnosis is a technical method that applies "dimensionless parameters" to equipment fault diagnosis. The dimensionless diagnosis parameters evolve from the dimensionless parameters, and their values are determined by the nature or shape of the probability density function of the signal amplitude, that is, the shape of the probability density function corresponding to different operating states is different. However, the change of working conditions, load and speed has no effect on the dimensionless index. These properties are very useful for the time domain analysis of fault diagnosis.

The dimensionless index is defined as follows:

$$\zeta_x = \frac{\left[\int_{-\infty}^{+\infty} |x|^l \, p(x)\mathrm{d}x\right]^{\frac{1}{l}}}{\left[\int_{-\infty}^{+\infty} |x|^m \, p(x)\mathrm{d}x\right]^{\frac{1}{m}}}, \tag{1}$$

where x represents the amplitude of vibration and $p(x)$ represents the probability density function of the amplitude of vibration. At present, the most commonly used dimensionless indicators include the waveform index, pulse index, margin index, peak index and kurtosis index. According to formula (1):

If $l = 2, m = 1$, there is the waveform index

$$S_f = \frac{\left[\int_{-\infty}^{+\infty} |x|^2 \, p(x)\mathrm{d}x\right]^{\frac{1}{2}}}{\left[\int_{-\infty}^{+\infty} |x| \, p(x)\mathrm{d}x\right]} = \frac{X_{rms}}{|\bar{X}|}. \tag{2}$$

If $l \to \infty, m = 1$, there is the pulse index

$$I_f = \frac{\lim\limits_{l\to\infty}\left[\int_{-\infty}^{+\infty} |x|^l \, p(x)\mathrm{d}x\right]^{\frac{1}{l}}}{\left[\int_{-\infty}^{+\infty} |x| \, p(x)\mathrm{d}x\right]} = \frac{X_{\max}}{|\bar{X}|}. \tag{3}$$

If $l \to \infty, m = \frac{1}{2}$, there is the margin index

$$CL_f = \frac{\lim\limits_{l\to\infty}\left[\int_{-\infty}^{+\infty}|x|^l\ p(x)\mathrm{d}x\right]^{\frac{1}{l}}}{\left[\int_{-\infty}^{+\infty}|x|^{\frac{1}{2}}\ p(x)\mathrm{d}x\right]^2} = \frac{X_{\max}}{X_r}. \tag{4}$$

If $l \to \infty, m = 2$, there is the peak index

$$C_f = \frac{\lim\limits_{l\to\infty}\left[\int_{-\infty}^{+\infty}|x|^l\ p(x)\mathrm{d}x\right]^{\frac{1}{l}}}{\left[\int_{-\infty}^{+\infty}|x|^2\ p(x)\mathrm{d}x\right]^{\frac{1}{2}}} = \frac{X_{\max}}{X_{rms}}. \tag{5}$$

If $l = 4, m = 2$, there is

$$N = \frac{\left[\int_{-\infty}^{+\infty}|x|^4\ p(x)\mathrm{d}x\right]^{\frac{1}{4}}}{\left[\int_{-\infty}^{+\infty}|x|^2\ p(x)\mathrm{d}x\right]^{\frac{1}{2}}}. \tag{6}$$

Define the kurtosis index

$$K_v = N^4 = \frac{\beta}{X_{rms}^4}. \tag{7}$$

2.2 Dimensionless immune diagnostic techniques

The specific steps for the production of a dimensionless index immune detector are as follows:

(1) After the operation of the new equipment and normal operation for a period of time, the corresponding space of each dimensionless index can be determined by calculating the monitoring data, thus forming the initial detector.

(2) Once the situation of non-self space is found through the initial detector, after confirming the fault type, the corresponding detection data corresponding to the coding string of the artificial immune detector are recorded to generate the mature detector.

(3) With the accumulation of data, after removing the repeated and crossed detection coding strings in the mature detector, the detection coding data corresponding to the fault type is formed to generate an excellent detector.

The intelligent fault diagnosis system separates the offline phase and the online phase. In the offline stage, the scope of dimensionless indexes under each fault is established by an artificial immune algorithm, an SVM model and a machine learning algorithm, mainly using historical monitoring data or the possible fault data of the equipment. The specific process is shown in Fig. 1.

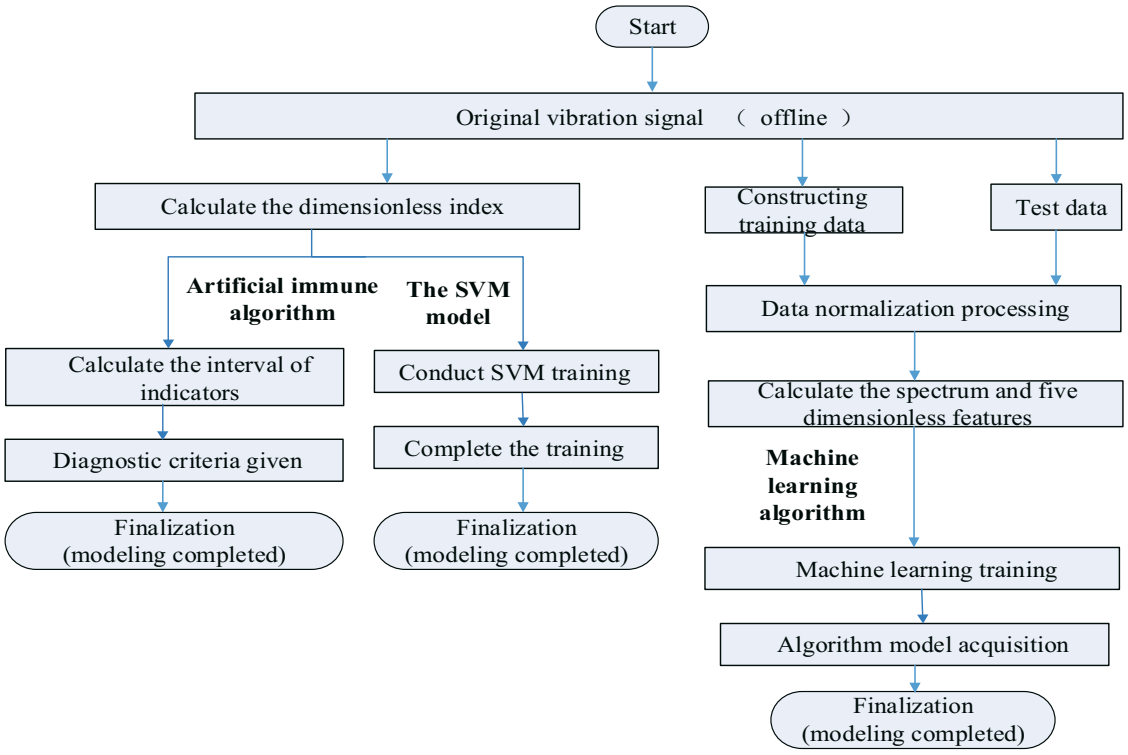

Fig. 1 Offline modeling flow chart

In the online stage, the dimensionless index is calculated by obtaining the actual online monitoring data. According to the dimensionless index range established in the offline stage, the artificial immune method is used to calculate the fault diagnosis results corresponding to each dimensionless index, and then the SVM model is used to give the fault type, and the classification prediction algorithm is used to predict the fault accuracy. The specific process is shown in Fig. 2.

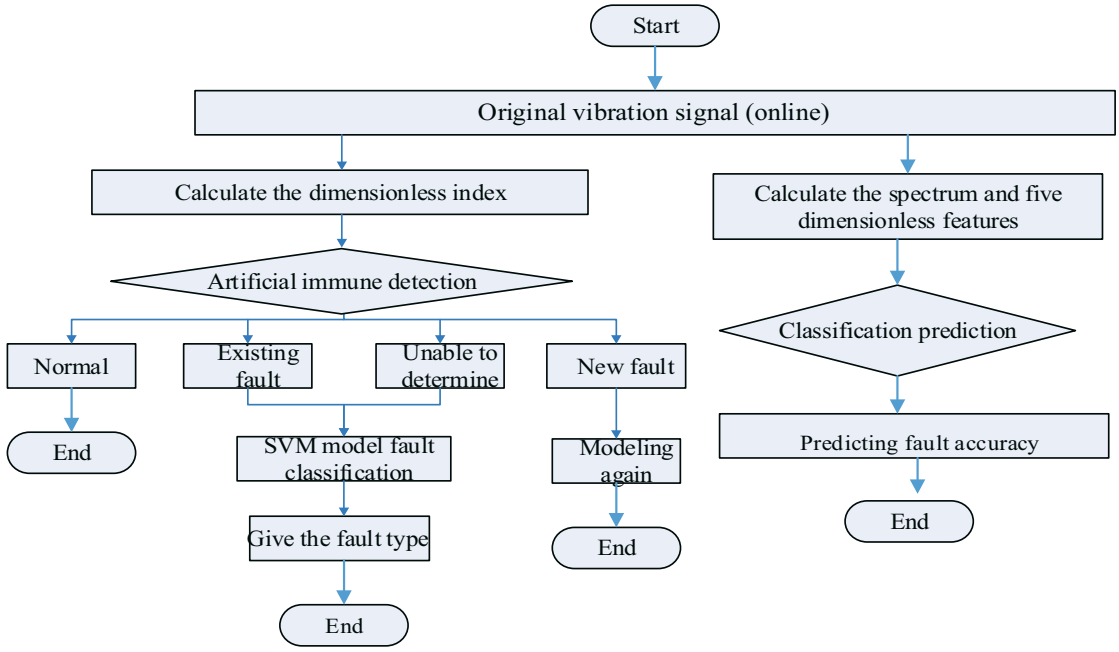

Fig. 2 Online modeling flow chart

For example, let us take the dimensionless features of normal and various fault states of the equipment (including a worn left bearing outer ring, a worn left bearing inner ring, the big gear is toothless, all the gears in the gearbox are missing teeth, the big gear is toothless +

missing a ball on the left bearing, the big gear is toothless + the left bearing inner ring is worn, and the big gear is toothless + the left bearing outer ring is worn) as a training set and a test set to build the model. The change of diagnostic effect with the proportion of training samples is shown in Table 1. It can be seen from Table 1 that the average accuracy increases gradually with the increase of the proportion of training samples. When the selection proportion is above 25%, the average accuracy is above 95%, where the average accuracy is the average accuracy of the 10 runs.

Table 1 Change of diagnostic accuracy with training sample ratio (10 runs)

TRAINING SAMPLE RATIO	OPTIMAL ACCURACY	AVERAGE ACCURACY	RUN TIME
15%	0.991	0.9063	52.947
25%	1	0.9501	99.841
35%	1	0.9706	141.9
45%	1	0.9786	195.628
55%	1	0.9845	246.08
65%	1	0.993	293.128
75%	1	0.9912	324.295

Eight fault types were tested in sequence, and 80 samples were used for each fault type for 10 cycles (800 tests were performed for each fault type). The average statistical diagnostic accuracy is shown in Table 2. As can be seen from Table 2, the average accuracy of the eight default fault diagnoses is 94.73%.

Table 2 Eight types of fault diagnosis accuracy

FAULT	Number of single test samples	Number of repeated tests	Number of successful diagnoses	Diagnostic accuracy
THE BIG GEAR IS TOOTHLESS	80	10	796	99.5%
The big gear is toothless + Left bearing outer ring worn	80	10	769	96.12%
The big gear is toothless + Left bearing inner ring is worn	80	10	695	86.87%
The big gear is toothless + Missing ball on left bearing	80	10	794	99.25%
All the gears in the gearbox are missing teeth	80	10	635	79.37%
Left bearing inner ring is worn	80	10	774	96.75%
Left bearing outer ring worn	80	10	800	100%
NORMAL	80	10	800	100%

3. Hardware constitution

The fault diagnosis system of rotating machinery stores, transmits and calculates the collected data, so as to accurately judge the fault diagnosis target of the rotating machinery. The system collects and processes the signal through the data collector. The server stores and manages the data, and also transmits and releases the data online. Through the remote network, the collected online measured data of large industrial field equipment of enterprise users are transmitted to the remote fault diagnosis centre. Then, using the intelligent diagnosis system of the compound faults of rotating machinery, the working state, development trend and characteristics of the compound faults of industrial field equipment can be further analysed to achieve the experimental verification and the application of research of the state trend prediction as well as the compound fault diagnosis of industrial field equipment.

To better achieve data collection, storage, operation and monitoring, the hardware of the industrial unit intelligent fault diagnosis device consisting of six speed sensors, one data collector, one server and one PC are designed. The system structure diagram is shown in Fig. 3.

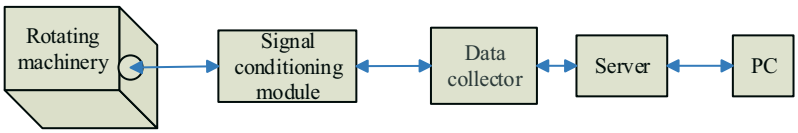

Fig. 3 System structure diagram

The system adopts six speed sensors installed on the shell and the bearing seat in three directions, namely horizontal, vertical and axial, to collect the vibration signal of the unit. The signal conditioning module amplifies the vibration signal. The data acquisition, storage and processing of the signal are carried out by the collector. The server is used for data storage and management, data online transmission and release. The PC is used for the diagnostic maintenance personnel to check the operation information of the unit at any time.

3.1 Vibration sensor selection

The speed sensor VE101-2D is selected as the sensor for signal acquisition. Its performance requirements are as follows: sensitivity 100mV/IPS ±10% (25℃); frequency response 1.5 ~ 12000Hz (±3dB) 2.0 ~ 4500Hz (±10%); maximum amplitude ±50in/ SEC PEAK; stabilization time <4.0s; power supply voltage: 18-30 VDC; constant current 2-4mA; output impedance <100 ohm; bias voltage 10 ~ 14VDC.

The vibration signal comes from the CTC speed sensor (Fig. 4), and the physical quantity of vibration speed is converted into an electrical signal for output.

Fig. 4 VE101-2D speed sensor

3.2 Signal conditioning module

The main functions of the signal conditioning module include generating the constant current source required by the vibration sensor, changing the vibration current signal into a

voltage signal and amplifying voltage signal. The signal conditioning module has the following indicators:

(1) The frequency width of the signal conditioning circuit is 1.5 ~ 12000Hz, the gain is 60dB, and the output amplitude SNR is greater than or equal to 30dB;

(2) The gain flatness of the amplifier is less than 3dB;

(3) It generates a 10mA stable constant current source with a current change rate of less than 2%;

(4) It is consistent with the voltage range, impedance and interface of the front-end acquisition sensor and the back-end signal filtering module.

The signal conditioning module is a low-noise signal amplifier, which provides accurate vibration signals for subsequent filtering and acquisition (Fig. 5).

Fig. 5 Signal conditioning module

3.3 Data collector

The data collector is responsible for data collection and pre-processing. It must be connected to a 220V AC power supply. The data collector will transmit the collected vibration signals to the data storage server through the network connection. At the same time, the installation and debugging of the system software can be done by connecting a USB mouse, USB keyboard and display. An illustration is shown in Fig. 6.

Fig. 6 Data collector

3.4 Server

The collected signals are entered into the system through a network connection for analysing and processing, and data sharing is achieved at the same time, which can be provided

to multiple clients for vibration signal monitoring and fault diagnosis analysis. Fig. 7 illustrates this.

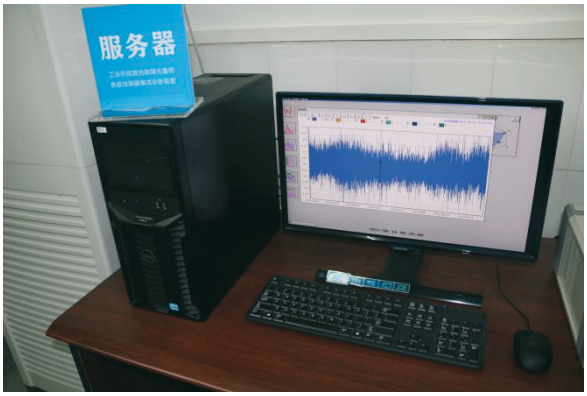

Fig. 7 Server

4. System interface design

4.1 Main interface

The main interface of the system consists of the following parts. The upper left corner is the name of the system. The left and right side parts show the vibration intensity of six measuring points and the real time value of five common dimensionless indicators.

Fig. 8 Main interface

Detailed description of indicators:

(1) Indicator name: now includes dimensionless vibration intensity and five dimensionless indicators (waveform index, peak index, margin index, pulse index, kurtosis index).

(2) Indicator value: the value calculated from the original waveform according to the above formula, and the three states of normal, attention and alarm are represented by green, yellow and red (thresholds are set for each indicator, and colour changes will be triggered if the threshold is exceeded).

(3) Collection time, the time of the data packets obtained by the collection system (the system will generally collect and diagnose within 5 seconds; if there is a large amount of computation, the time interval of the system update data may be greater than 5 seconds).

4.2 Waveform and spectrum of vibration

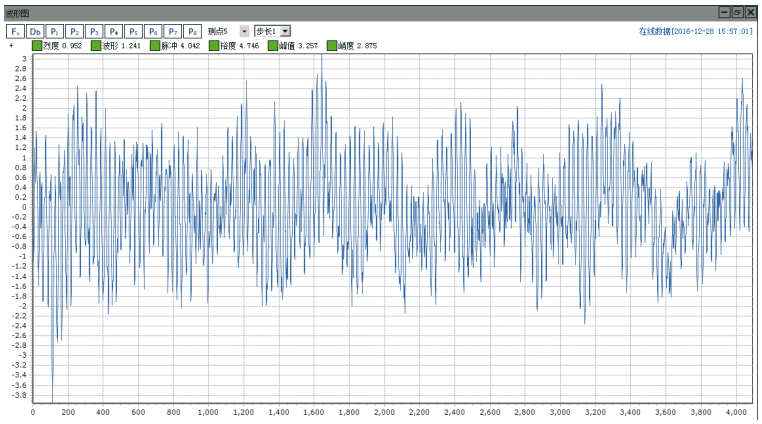

Fig. 9 Real time waveform

(1) Function: display a real-time vibration waveform and various index values.

(2) Vibration intensity: if the calculated vibration intensity value exceeds the alarm threshold, the colour of the calculated value and the alarm colour box will turn yellow or red.

(3) Dimensionless index: including waveform index, peak index, pulse index, margin index and kurtosis index, display index calculated value.

(4) Indicator alarm: indicator value is shown in green, yellow and red according to the alarm threshold (normal, attention, alarm).

(5) Vibration waveform: the vibration waveform curve collected and digitized by the collector. The abscissa is the sampling sequence number, and the ordinate is the millivolt voltage. The curve is refreshed according to the real-time data, and 4000 data points are displayed for each channel.

(6) Waveform zooming: click the left mouse button on the drawing to select an area from the top left to the bottom right direction to enlarge the curve of the area.

(7) Spectrum: including power spectrum, logarithmic power spectrum, power cepstrum, amplitude spectrum, amplitude cepstrum, phase spectrum, envelope spectrum and maximum entropy.

4.3 Trend chart

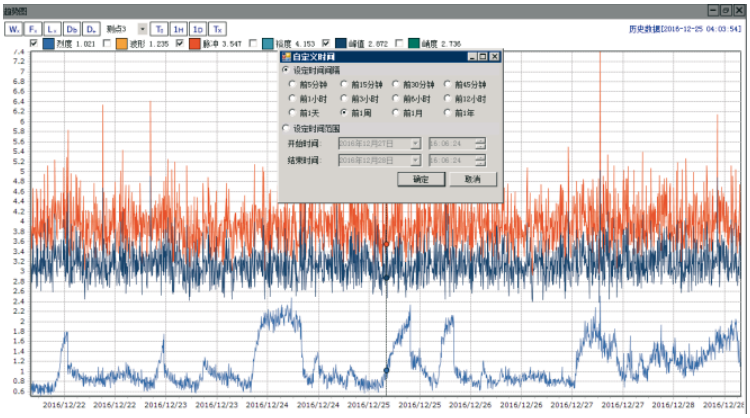

Fig. 10 Trend chart

(1) Function: query real-time trend and historical data curves of multiple indicators over a period of time.

(2) Select a time range: refer to the instructions in the main toolbar above for starting and ending times.

(3) Indicator toolbar: the toolbar located at the top is used to select the indicator items. More than one can be selected. Only the selected indicator will be displayed with the data line.

(4) Hide and show the index curve: click or cancel the check box in the middle of the trend chart, and the index curve corresponding to the check box will show and hide the index data line as optional or not optional.

(5) Query data: click this button to trigger a query operation, and the curve on the interface will be updated according to the selected index and time range.

(6) Vibration waveform: display the vibration waveform curve in the historical data. The abscissa is the sampling sequence number and the ordinate is the millivolt voltage. The curve is refreshed according to the real-time data.

(7) Waveform zooming: click the left mouse button on the drawing to select an area from the top left to the bottom right direction to enlarge the curve of the area.

4.4 Data list

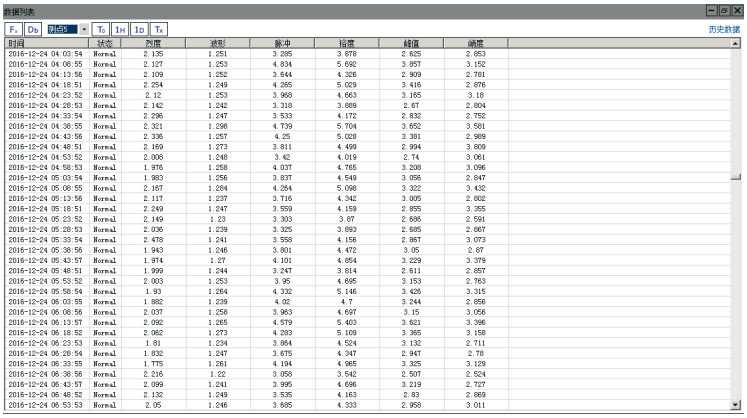

时间	状态	烈度	波形	脉冲	裕度	峭度	峰度
2016-12-24 04:03:54	Normal	2.135	1.251	3.285	3.878	2.625	2.853
2016-12-24 04:08:55	Normal	2.127	1.253	4.834	5.692	3.857	3.152
2016-12-24 04:13:56	Normal	2.109	1.252	3.644	4.326	2.909	2.781
2016-12-24 04:18:51	Normal	2.254	1.249	4.265	5.029	3.416	2.876
2016-12-24 04:23:52	Normal	2.12	1.253	3.958	4.663	3.165	3.18
2016-12-24 04:28:53	Normal	2.142	1.242	3.318	3.889	2.67	2.804
2016-12-24 04:33:54	Normal	2.296	1.247	3.533	4.172	2.832	2.752
2016-12-24 04:38:55	Normal	2.321	1.298	4.739	5.704	3.652	3.581
2016-12-24 04:43:56	Normal	2.336	1.257	4.25	5.028	3.381	2.969
2016-12-24 04:48:51	Normal	2.169	1.273	3.811	4.499	2.994	3.009
2016-12-24 04:53:52	Normal	2.008	1.248	3.42	4.019	2.74	3.061
2016-12-24 04:58:53	Normal	1.976	1.258	4.037	4.765	3.208	3.096
2016-12-24 05:03:54	Normal	1.983	1.256	3.837	4.549	3.056	2.847
2016-12-24 05:08:55	Normal	2.157	1.284	4.264	5.098	3.322	3.432
2016-12-24 05:13:56	Normal	2.117	1.237	3.716	4.342	3.005	2.802
2016-12-24 05:18:51	Normal	2.249	1.247	3.559	4.159	2.855	3.355
2016-12-24 05:23:52	Normal	2.149	1.23	3.303	3.87	2.695	2.591
2016-12-24 05:28:53	Normal	2.036	1.239	3.325	3.893	2.685	2.867
2016-12-24 05:33:54	Normal	2.478	1.241	3.558	4.156	2.867	3.073
2016-12-24 05:38:56	Normal	1.943	1.246	3.801	4.472	3.05	2.87
2016-12-24 05:43:57	Normal	1.974	1.27	4.101	4.854	3.229	3.379
2016-12-24 05:48:51	Normal	1.999	1.244	3.247	3.814	2.611	2.857
2016-12-24 05:53:52	Normal	2.003	1.253	3.95	4.695	3.153	2.763
2016-12-24 05:58:54	Normal	1.93	1.264	4.332	5.146	3.426	3.315
2016-12-24 06:03:55	Normal	1.882	1.239	4.02	4.7	3.244	2.856
2016-12-24 06:08:56	Normal	2.037	1.258	3.963	4.697	3.15	3.056
2016-12-24 06:13:57	Normal	2.092	1.265	4.579	5.403	3.621	3.396
2016-12-24 06:18:52	Normal	2.062	1.273	4.283	5.109	3.365	3.158
2016-12-24 06:23:53	Normal	1.81	1.234	3.864	4.524	3.132	2.711
2016-12-24 06:28:54	Normal	1.832	1.247	3.675	4.347	2.947	2.78
2016-12-24 06:33:55	Normal	1.775	1.261	4.194	4.965	3.325	3.129
2016-12-24 06:38:56	Normal	2.216	1.22	3.058	3.542	2.507	2.524
2016-12-24 06:43:57	Normal	2.099	1.241	3.995	4.696	3.219	2.727
2016-12-24 06:48:52	Normal	2.132	1.249	3.535	4.163	2.83	2.869
2016-12-24 06:53:53	Normal	2.05	1.246	3.695	4.333	2.958	3.011

Fig. 11 Data list

(1) Function: display historical data records within a period of time, including channel number, time point, state, vibration intensity, waveform index, peak index, margin index, pulse index, kurtosis index.

(2) Query data: clicking this button to execute the query will display historical data for the selected channel and time range.

(3) Time: the point in time corresponding to the history record.

(4) Indicator value: the calculation value of vibration intensity, waveform index, peak index, margin index, pulse index and kurtosis index.

5. A case study

Through the vibration amplitude diagram of a petrochemical enterprise – air separation device – air compressor B unit – steam turbine (as shown in Fig. 12), 50 groups of original vibration waveform data, a total of 150 groups, were derived from the system respectively in the time period of stable vibration and the time period of two vibration protrudes. The sampling points of each group of data were 1024. Normal and failure are classified according to five dimensionless indicators, and the results are shown in Fig. 13.

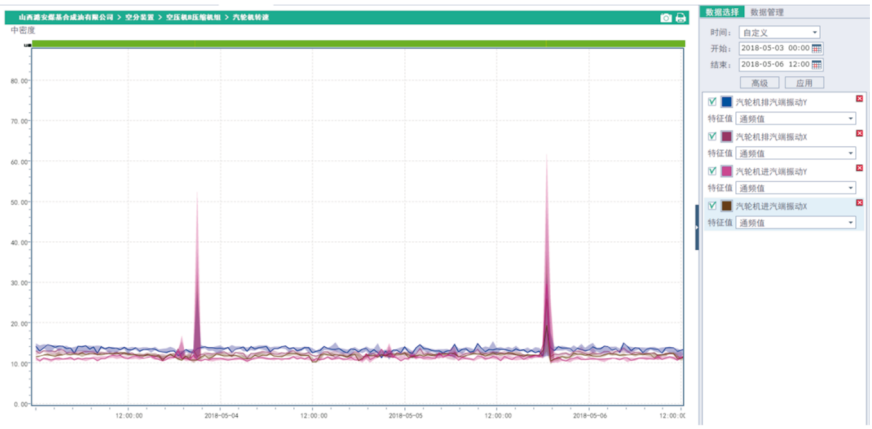

Fig. 12 Amplitude diagram

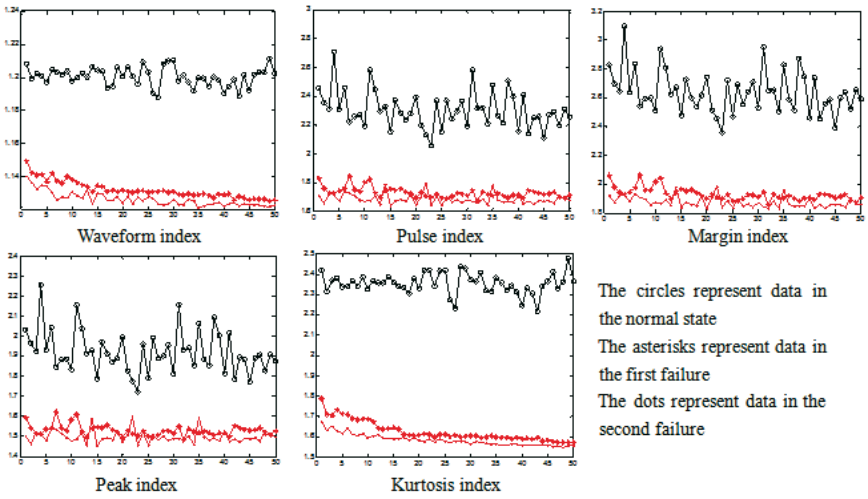

Fig. 13 Dimensionless index classification rendering

Through the analysis of the above five dimensionless index graphs, it is clear that the five dimensionless indexes can distinguish the normal state from the fault state, and all of them can judge when the failure of the unit occurs. As for the fault type, the dimensionless immune ensemble diagnosis algorithm is used to model the normal state data and the fault data of the first occurrence, and then to determine the fault type of the second occurrence. According to the diagnosis model, the type of the second fault is consistent with the type of the first fault.

6. Conclusion

This paper introduces an intelligent fault diagnosis system based on a dimensionless immune detector and an SVM. The system is designed with dimensionless immune detectors, combined with the SVM and a machine learning algorithm. Not only does it have high diagnostic accuracy, but it can also achieve real-time, online, fast and remote fault diagnosis. Therefore, the effective operation of the system plays an important role in the safe production of large rotating machinery units and in avoiding safety accidents and has obtained good social and economic benefits.

At present, for an intelligent fault diagnosis system, the following problems remain to be solved:

(1) The number of dimensionless indexes available is limited, and the number of dimensionless indexes applied to multiple concurrent fault diagnosis is even less.

(2) The problem of how to establish a time-frequency domain fusion intelligent fault diagnosis system suitable for the health management of the whole life cycle of rotating machinery for all kinds of faults of different equipment in the early, middle and late stages.

Acknowledgments

The research was partially supported by the Key Project of Natural Science Foundation of China (Grant No. 61933013) and the National Nature Science Foundation of China (Grant No. 62073090). The work described in this paper was also partially supported by the Natural Science Foundation of Guangdong (Grant No. 2019A1515010700) .

REFERENCES

[1] Q. H. Zhang, A. S. Qin, L. Shu, G. X. Sun, L. Q. Shao. Vibration sensor based intelligent fault diagnosis system for large machine unit in petrochemical industries [J]. *International Journal of Distributed Sensor Networks*, vol. 2015, Article ID 239405, 13 pages, 2015. https://doi.org/10.1155/2015/239405

[2] Q. H. Zhang, Q. Hu, G. X. Sun, X. S. Si, A. S. Qin. Concurrent fault diagnosis for rotating machinery based on vibration sensors [J]. *International Journal of Distributed Sensor Networks*. 75(8): 93-102, 2013.

[3] J. B. Xiong, Q. H. Zhang, Z. P. Peng, G. X. Sun, W. C. Xu, Q. Wang. A diagnosis method for rotation machinery faults based on dimensionless indexes combined with K-Nearest neighbor algorithm [J]. *Mathematical Problems in Engineering*, vol. 2015, Article ID 563954, 9 pages, 2015. https://doi.org/10.1155/2015/563954.

[4] CEN Jian, XU Bu-gong, ZHANG Qing-hua, SHAO Long-qiu. Complex fault diagnosis of machine unit based on evidence theory and immune detector integrated [J]. *Control and Decision*, 26(8): 1248-1258, 2011.

[5] HU Chang-hua, SI Xiao-sheng, ZHOU Zhi-jie, WANG Peng. An improved D-S algorithm under the new measure criteria of evidence conflict [J]. *Acta electronica sinica*, 37(7): 1578-1583, 2009.

[6] A. Ashari, R. Nikoukhah, and S. Campbell. Active robust fault detection in closed-loop systems: Quadratic optimization approach [J]. *IEEE Trans. Autom. Control*, 57(10): 2532-2544, 2012. https://doi.org/10.1109/TAC.2012.2188430

[7] A. Grastien, A. Anbulagan. Diagnosis of discrete event systems using satisfiability algorithms: A theoretical and empirical study [J]. *IEEE Trans. Autom. Control*, 58(12): 3070-3083, 2013. https://doi.org/10.1109/TAC.2013.2275892

[8] A. Soualhi, G. Clerc, H. Razik. Detection and diagnosis of faults in induction motor using an improved artificial ant clustering technique [J]. *IEEE Trans. Ind. Electron*., 60(9): 4053–4062, 2013. https://doi.org/10.1109/TIE.2012.2230598

[9] Grzegorz Królczyk, Zhixiong Li and Jose Alfonso Antonino Daviu. Fault diagnosis of rotating machine[J]. *Applied Sciences*. 2020, 10, 1961. https://doi.org/10.3390/app10061961

[10] J. B. Xiong, Q. H. Zhang, G. X. Sun, Z. P. Peng, Q. Liang. Fusion of the dimensionless parameters and filtering methods in rotating machinery fault diagnosis [J]. *Journal of Networks*, 9(5): 1201-1207, 2014.

[11] Q. Sun, X. Ye, W. K. Gu. A new combination rules of evidence theory [J]. *Acta electronica sinica*, 28(8): 117-119, 2000.

[12] Cui Delong, Zhang Qinghua, Xiao Ming, Wang Lei. Feature spectrum extraction algorithm for rolling bearings based on spectrogram and constrained NMF [J]. *Bearing*, 5: 48-52, 2014.

[13] X. Dai, Z. Gao. From model, signal to knowledge: A data-driven perspective of fault detection and diagnosis [J]. *IEEE Trans. Ind. Informat*., 9(4): 2226-2238, 2013. https://doi.org/10.1109/TII.2013.2243743

[14] X. S. Si, C. H. Hu, J. B. Yang. On the dynamic evidential reasoning approach for fault prediction [J]. Expert Systems with Applications, 38(5): 5061-5080, 2011. https://doi.org/10.1016/j.eswa.2010.09.144

[15] SUN Guo-xi, ZHANG Qing-hua, WEN Cheng-lin, DUAN Zhi-hong. Astochastic degradation modeling based adaptive prognostic approach for equipment [J]. *Acta electronica sinica*, 6: 1119-1126, 2015.

[16] Q. H. Zhang, A. S. Qin, L. Shu, G. X. Sun, L. Q. Shao. Vibration sensor based intelligent fault diagnosis system for large machine unit in petrochemical industries [J]. *International Journal of Distributed Sensor Networks*, in press, 2016. https://doi.org/10.1155/2015/239405

[17] Lu N, Wang S, Xiao H. An unsupervised intelligent fault diagnosis system based on feature transfer [J]. *Mathematical Problems in Engineering*, 2021, 2021(4):1-12. https://doi.org/10.1155/2021/6686057

[18] Wang X, Wang J, Privault M. Artificial intelligent fault diagnosis system of complex electronic equipment[J]. *Journal of Intelligent and Fuzzy Systems*, 2018, 35(4):1-11. https://doi.org/10.3233/JIFS-169735

[19] Hu J, Zhang L, Cai Z, et al. An intelligent fault diagnosis system for process plant using a functional HAZOP and DBN integrated methodology[J]. *Engineering Applications of Artificial Intelligence*, 2015, 45(OCT.):119-135. https://doi.org/10.1016/j.engappai.2015.06.010

[20] Hao G Y, Cheng J, Zong G Z, et al. Distributed monitoring and intelligent fault diagnosis system for large-scale electro-hydraulic devices [J]. *Applied Mechanics & Materials*, 2015, 779:163-168. https://doi.org/10.4028/www.scientific.net/AMM.779.163

Submitted: 29.7.2021

Accepted: 10.01.2022

Mr. Longqiu Shao*
Prof. Qinghua Zhang
Mr. Gaowei Lei
Mr. Naiquan Su
Mr. Penghui Yuan
School of Automation, Guangdong
University of Petrochemical Technology
Maoming 525000, China
*Corresponding author:
845338290@qq.com